

# Sensitive search for the temporal variation of the fine structure constant using radio-frequency E1 transitions in atomic dysprosium

A. T. Nguyen\*

*Department of Physics, University of California at Berkeley, Berkeley, California 94720-7300*

D. Budker†

*Department of Physics, University of California at Berkeley, Berkeley, California 94720-7300 and  
Nuclear Science Division, Lawrence Berkeley National Laboratory, Berkeley, California 94720*

S. K. Lamoreaux‡ and J. R. Torgerson§

*University of California, Los Alamos National Laboratory,  
Physics Division, P-23, MS-H803, Los Alamos, New Mexico 87545*

(Dated: May 22, 2019)

It has been proposed that the radio-frequency electric-dipole (E1) transition between two nearly degenerate opposite-parity states in atomic dysprosium should be highly sensitive to possible temporal variation of the fine structure constant ( $\alpha$ ) [V. A. Dzuba, V. V. Flambaum, and J. K. Webb, *Phys. Rev. A* **59**, 230 (1999)]. We discuss here an experimental realization of the proposed search, which involves monitoring the E1 transition frequency over a period of time using direct frequency counting techniques. We estimate that a statistical sensitivity of  $|\dot{\alpha}/\alpha| \sim 10^{-18}/\text{yr}$  may be achieved and discuss possible systematic effects in such a measurement.

PACS numbers: PACS. 06.20.Jr, 32.30.Bv

## I. INTRODUCTION

Temporal variation of the fundamental constants of nature would signify new physics beyond the Standard Model, as discussed in a recent review [1]. Various theories constructed to unify gravity with the other forces allow or necessitate such a variation [2, 3, 4, 5]. Of recent interest is the astrophysical evidence for a variation of the fine structure constant  $\alpha$ . From an analysis of quasar absorption spectra [6] over the redshift range  $.5 < z < 3.5$ , a  $4\sigma$  deviation of  $\Delta\alpha/\alpha = (-0.72 \pm 0.18) \times 10^{-5}$  from zero was reported. Assuming a linear shift over  $\sim 10^{10}$  years, this corresponds to a temporal variation of  $\dot{\alpha}/\alpha = (-7.2 \pm 1.8) \times 10^{-16}/\text{yr}$ . This value seems to disagree significantly with the current best terrestrial limit of  $|\dot{\alpha}/\alpha| < 10^{-18}/\text{yr}$  [7, 8, 9], which comes from an analysis of geophysical data obtained from a natural fission reaction which took place  $1.8 \times 10^9$  years ago at the Oklo uranium mine in Gabon. Observational measurements like these, however, are subject to numerous assumptions which tend to complicate the interpretation.

Laboratory searches have numerous advantages, but have, thus far, placed weaker limits on  $\dot{\alpha}/\alpha$ . For example, a comparison between Rb and Cs microwave clocks yielded  $|\dot{\alpha}/\alpha| \leq 1.1 \times 10^{-14}/\text{yr}$  [10] while a similar comparison between H-maser and  $\text{Hg}^+$  gave  $\dot{\alpha}/\alpha \leq 3.7 \times 10^{-14}/\text{yr}$  [11]. More recently, a significantly tighter

limit of  $|\dot{\alpha}/\alpha| < 1.2 \times 10^{-15}/\text{yr}$  was obtained from a comparison of a  $\text{Hg}^+$  optical clock to a Cs microwave clock [12] using a frequency comb.

It has been suggested [13, 14] that the electric-dipole (E1) transition between two nearly degenerate opposite-parity states in atomic dysprosium (Dy;  $Z=66$ ) should be highly sensitive to variations in  $\alpha$ . Indeed, a recent calculation [15] supports this conclusion. An experimental search utilizing these states is currently underway and is discussed here. We provide an analysis of possible systematic effects and show that this search could ultimately reach a sensitivity of  $|\dot{\alpha}/\alpha| \sim 10^{-18}/\text{yr}$ .

## II. VARIATION OF ALPHA IN DYSPROSIUM

Tests of variation of  $\alpha$  in atomic systems rely upon the fact that relativistic corrections depend differently on  $\alpha$  for different energy levels. The total energy of a level can be written as

$$E = E_0 + q(\alpha^2/\alpha_0^2 - 1) + \mathcal{O}(\alpha^3), \quad (1)$$

where  $E_0$  is the present-day energy,  $\alpha_0$  is the present-day value of the fine structure constant, and  $q$  is a coefficient which determines the sensitivity to variations of  $\alpha$ . This coefficient mainly depends upon the electronic configuration of the level. A recent calculation [15], utilizing relativistic Hartree-Fock and configuration interaction methods, found values of  $q$  for two nearly degenerate opposite-parity states in atomic dysprosium that are both large and of opposite sign. For the even-parity state (designated as A),  $q_A/hc = 6008 \text{ cm}^{-1}$  while, for the odd-parity state (designated as B),  $q_B/hc = -23708 \text{ cm}^{-1}$ .

\*Electronic address: atn@socrates.berkeley.edu

†Electronic address: budker@socrates.berkeley.edu

‡Electronic address: lamore@lanl.gov

§Electronic address: torgerson@lanl.gov

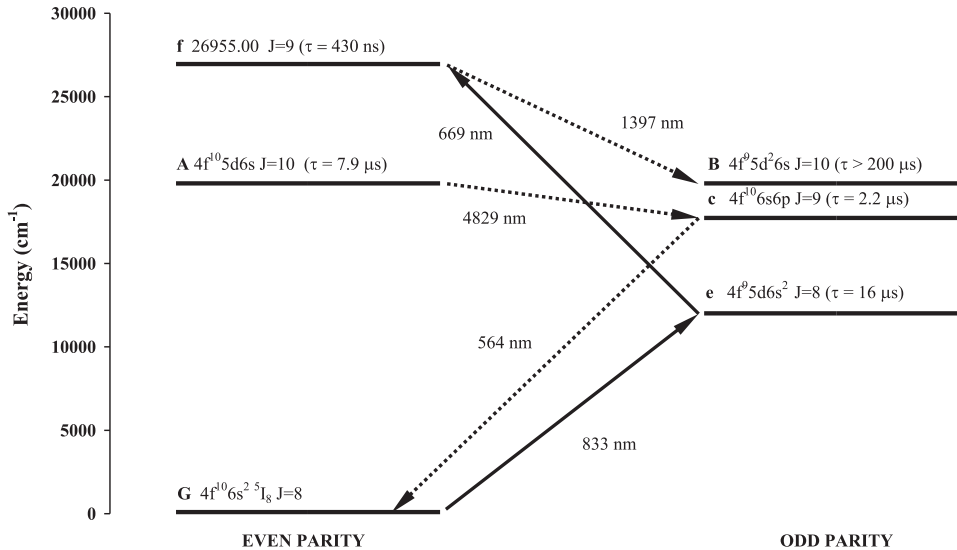


FIG. 1: Partial energy-level diagram of dysprosium showing the present scheme to populate level B and detect the population of level A. Solid lines: absorption. Dashed lines: spontaneous emission.

The time variation of the transition frequency between levels A and B becomes (for  $\alpha \approx \alpha_0$ )

$$|\dot{\nu}| = 2 \frac{|q_A - q_B|}{h} \left| \frac{\dot{\alpha}}{\alpha_0} \right| \sim 2 \times 10^{15} \text{ Hz} \left| \frac{\dot{\alpha}}{\alpha} \right|. \quad (2)$$

In other words,  $|\dot{\alpha}/\alpha| = 10^{-15}/\text{yr}$ , implies  $|\dot{\nu}| = 2 \text{ Hz/yr}$ .

The statistical uncertainty of determining the central frequency from a resonance lineshape is  $\delta\nu \sim \gamma/\sqrt{N}$ , where  $N$  is the number of counts and  $\gamma$  is the transition width. In the dysprosium system,  $\gamma = 20 \text{ kHz}$  is determined mainly from the lifetime of state A,  $\tau_A = 7.9 \mu\text{s}$  ( $\tau_B > 200 \mu\text{s}$ ) [16]. A reasonable counting rate of  $10^9 \text{ s}^{-1}$ , corresponds to a statistical sensitivity to  $\nu_0$  of  $\sim 0.6 \tau^{-1/2} \text{ Hz}\sqrt{\text{s}}$  where  $\tau$  is the integration time in seconds. After an integration time of one day,  $\delta\nu \sim 2 \text{ mHz}$ , thus allowing for a sensitivity of  $|\dot{\alpha}/\alpha| \sim 10^{-18}/\text{yr}$  for two measurements separated by a year's time.

### III. EXPERIMENTAL TECHNIQUE

#### A. Overview

The experimental search for a variation of the E1 transition frequency between the two opposite-parity states will proceed as follows. As shown in Fig. 1, atoms are populated [17] to the longer-lived odd-parity state B ( $\tau_B > 200 \mu\text{s}$  [16]) via three transitions. The first two transitions require light at 833 nm and 669 nm, respec-

It should be noted that unlike experiments involving optical frequencies, the sensitivity to a variation in  $\alpha$  is not proportional to  $\delta\nu/\nu$ . The reason is that if  $\nu$  is small enough, the uncertainty in its determination is no longer limited by the relative uncertainty of the reference clock frequency ( $\nu_{\text{clock}}$ ), but rather by other experimental uncertainties. For example, a modest Cs clock provides an absolute accuracy of  $10^{-12}$ . In the Dy transitions considered here, typical frequencies are  $\sim 1 \text{ GHz}$  or smaller. Thus the clock uncertainty will only become an issue when other uncertainties can be reduced to the level of

$$\nu \frac{\delta\nu_{\text{clock}}}{\nu_{\text{clock}}} \sim 10^{-3} \text{ Hz}. \quad (3)$$

and even then can be overcome in a straightforward way by using a better reference clock.

tively. The third transition involves spontaneous decay with a branching ratio of 30% and the emission of 1397-nm light. Once in state B, atoms are transferred to state A with an rf electric field, whose frequency is referenced to a commercial Cs frequency standard. A resonance lineshape is attained by scanning the rf frequency and monitoring 564-nm light from the second step of fluorescence from state A.

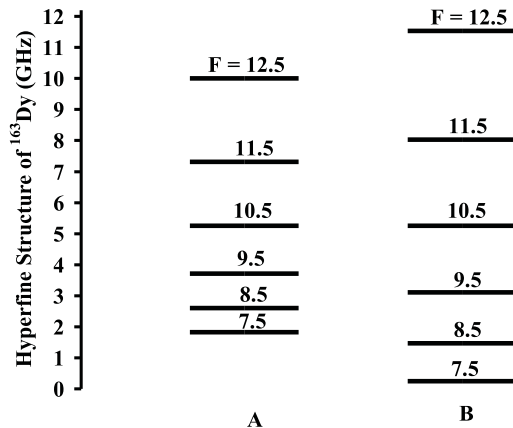


FIG. 2: Hyperfine structure of A & B levels of  $^{163}\text{Dy}$ . Zero energy is chosen for the lowest hyperfine component.

### B. rf transitions

Because the energy separation between the nearly degenerate levels is on the order of hyperfine splittings and isotope shift energies (Fig. 2), and because dysprosium has seven stable isotopes, there are many choices of rf frequencies. Table I shows a table of rf frequencies below 2 GHz calculated from measured hyperfine constants and isotope shifts [16]. The smallest transition frequency (3.1 MHz) occurs for the  $F = 10.5$  components of  $^{163}\text{Dy}$  (the same transition is used in a search for parity nonconservation (PNC) [18]). The lowest transition frequency that offers a high counting rate is the 235 MHz transition in  $^{162}\text{Dy}$ . This is because of a large isotopic abundance and the fact that there are no hyperfine levels to dilute the atomic population. As discussed below, the choice of rf transition is also important in regard to sensitivity to systematic effects.

### C. Apparatus

We have studied states A and B extensively as a system to measure atomic PNC effects [18]. Although our current apparatus is optimized for a PNC experiment, it is suitable for a measurement of  $\dot{\alpha}$  with only minor modifications. We describe this system here in order to make a realistic evaluation of a possible experiment.

An atomic beam is produced by an effusive oven operating at 1500 K. The atoms pass through collimators and approach the interaction region (Fig. 3) where the desired electric and magnetic fields are produced. Inside the interaction region, the atoms encounter the laser beams used in the population scheme. The rf electric field is formed between two wire grids, which are used in order to minimize surface area and thus stray charge accumulation. Typical electric field amplitudes are  $\sim 5$  V/cm. If necessary, a magnetic field of up to  $\sim 4$  G can be applied. It is produced by eight turns of gold-plated

TABLE I: Calculated E1 transition frequencies using the hyperfine constants and isotope shifts from [16]. ( $\|d_J\| = 1.5(1) \times 10^{-2} \text{ ea}_0 \approx 19 \text{ kHz}/(\text{V}/\text{cm})$ )

$\nu_{rf}$ (MHz)	$\ d_F\ /\ d_J\ $	Isotope	$F_A$	$F_B$
-1328.6	1.00	160	10	10
-1856.4	0.15	161	7.5	8.5
-1714.7	1.04	161	11.5	11.5
-1249.7	0.99	161	10.5	10.5
-962.3	0.15	161	12.5	11.5
-791.5	0.94	161	9.5	9.5
-349.2	0.89	161	8.5	8.5
-172.7	0.19	161	11.5	10.5
68.9	0.86	161	7.5	7.5
514.0	0.20	161	10.5	9.5
1096.9	0.19	161	9.5	8.5
1576.0	0.15	161	8.5	7.5
-234.7	1.00	162	10	10
-1967.8	0.15	163	12.5	11.5
-1581.3	0.86	163	7.5	7.5
-1134.9	0.89	163	8.5	8.5
-609.7	0.94	163	9.5	9.5
-363.2	0.15	163	7.5	8.5
3.1	0.99	163	10.5	10.5
504.6	0.19	163	8.5	9.5
713.1	1.04	163	11.5	11.5
1531.0	1.10	163	12.5	12.5
1543.9	0.20	163	9.5	10.5
753.5	1.00	164	10	10

copper wire surrounding the interaction region. The entire interaction region is placed inside a magnetic shield. As atoms decay from state A, 564-nm light from the second step of fluorescence (Fig. 1) is collected by a light pipe and detected by a photomultiplier tube. The extent of the light pipe area is shown by the dashed box in Fig. 3.

Resonance lineshapes (Fig. 4) have recently been attained with this apparatus. Here, a magnetic field is scanned in the presence of a dc electric field revealing Zeeman-level-crossing resonances for  $^{163}\text{Dy}$ . For the measurement of  $\dot{\alpha}$ , the signal-to-noise will be much greater as individual Zeeman resonances will not be resolved.

The interaction region can be improved by making it shorter, as most atoms decay within twice the lifetime of state A ( $\tau_A = 7.9 \mu\text{s}$ ). Given a mean atomic velocity of  $5 \times 10^4 \text{ cm/s}$ , an appropriate length will be  $\sim 8 \text{ mm}$ . Furthermore, a shorter interaction region will allow for improved light collection efficiency, better suppression of

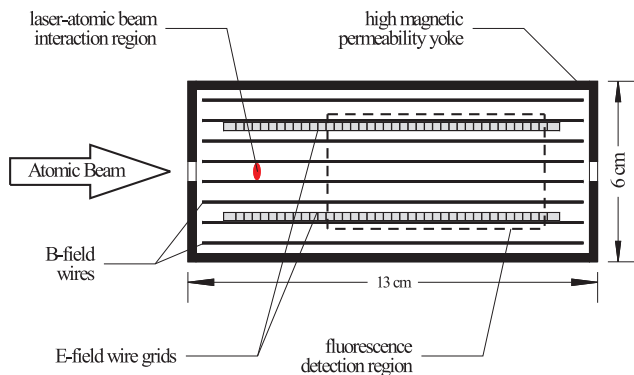


FIG. 3: Side view of interaction region currently optimized for PNC search.

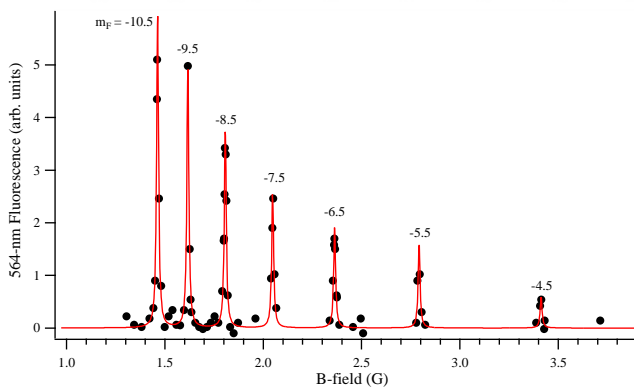


FIG. 4: Zeeman-level-crossing resonances for  $^{163}\text{Dy}$ . State B is populated as shown in Fig. 1 in the presence of an electric field of 0.4 V/cm. The population of state A, resulting from electric field-induced mixing of states A and B, is monitored by observing 564-nm fluorescence (Fig. 1). The solid line represents the best curve fit using the appropriate initial level separation and g-values measured in [16].

background oven light, and better control over E- and B-fields.

#### D. Lineshape

So long as the resonance is symmetrical, its exact shape is not important in the determination of the central frequency. The natural lineshape is a Lorentzian with a width ( $\gamma \approx 20$  kHz) determined mainly by the lifetime of state A ( $\tau_A = 7.9 \mu\text{s}$ ). To a first approximation, both transit-time and Doppler broadening change the lineshape in a symmetrical fashion. For an interaction length  $\sim 10$  cm and a mean atomic velocity of  $v = 5 \times 10^4$  cm/s, the transit-time width is  $\sim 5$  kHz. The Doppler width is  $\sim \nu(v/c)$ . For a 1 GHz transition, the Doppler width is  $\sim 2$  kHz. Thus, both transit-time and Doppler broadening contribute widths that are much smaller than the natural linewidth.

For an asymmetrical resonance, knowledge of the lineshape is only necessary if the asymmetry changes over time, i.e. there will be an apparent shift of the central frequency between measurements. In the following section, we discuss mechanisms leading to possible lineshape asymmetry and estimate the corresponding shifts.

## IV. SYSTEMATIC EFFECTS

High statistical sensitivity implies that our technique will likely be limited by how well we can control systematic effects. Below we analyze possible systematics and give estimates of how well various parameters of the experiment need to be controlled in order to achieve a sensitivity of  $|\dot{\alpha}/\alpha| \sim 10^{-18}/\text{yr}$ .

### A. dc Stark and quadrupole shifts

Variations of a stray dc electric field ( $E_{dc}$ ) can give rise to time-varying frequency shifts for the transition frequency between states  $m$  and  $n$ :

$$\delta\nu_{dc} = \sum_{j \neq m} \frac{d_{mj}^2 E_{dc}^2}{\Delta_{mj}} - \sum_{k \neq n} \frac{d_{nk}^2 E_{dc}^2}{\Delta_{nk}}, \quad (4)$$

where  $d_{mj}$  and  $\Delta_{mj} = E_m - E_j$  are the dipole matrix element and energy separation, respectively, between states  $m$  and  $j$ . The sum in Eq. (4) is taken over all states including hyperfine levels in the case of an odd isotope.

The reduced dipole matrix element for the A  $\rightarrow$  B transition is  $||d_J|| = 1.5(1) \times 10^{-2} e a_0 \approx 19$  kHz/(V/cm) [16]. For large  $J$ , the maximum z projection of the dipole moment  $\approx ||d_J||/\sqrt{2J} = 4$  kHz/(V/cm). Matrix elements connecting all levels with the same configurations as A and B have similar values [19]. As it turns out, between levels within  $2000 \text{ cm}^{-1}$  of the A and B levels, dipole matrix elements are relatively small, which reduces the sensitivity to systematics related to stray electric fields.

In an earlier PNC search, we reported stray dc E-fields of typically 50 mV/cm [18]. Using this value for the field and  $d \sim 4$  kHz/(V/cm), we estimate the shift for transition frequencies in the range 3 – 1000 MHz to be  $\sim 10^{-4} - 10^{-2}$  Hz. The stray electric field can also be measured at a few mV/cm level using the atoms themselves [18] and cancelled by the application of an external electric field.

An important systematic in  $\text{Hg}^+$  optical clock experiments [20] is the electric quadrupole shift due to a stray-field gradient ( $\nabla E$ ). Based upon the size of the interaction region and the homogeneity of the electric field ( $10^{-3}$ ) [18], a conservative estimate gives  $\nabla E \sim 10$  mV/cm<sup>2</sup>. Assuming a typical a quadrupole moment  $Q \sim 1 e a_0^2$  leads to a quadrupole shift estimated to be  $\lesssim 10^{-5}$  Hz and is thus negligible.

## B. ac Stark shift

Fluctuations of the rf electric-field amplitude ( $E$ ) can also lead to time-varying shifts. The ac Stark shift for a two-level system is given by:

$$\delta\nu_{ac} = \frac{d^2 E^2}{2(\Delta - \nu)} + \frac{d^2 E^2}{2(\Delta + \nu)}, \quad (5)$$

where  $\nu$  is the applied rf frequency,  $d$  is the dipole matrix element, and  $\Delta$  is the energy separation. Because the first term is an odd function of detuning, only the second so-called Bloch-Siegert term contributes to an actual shift of the central frequency of the resonance lineshape. For a saturated transition, we have  $d^2 E^2 / \gamma^2 \sim 1$  and  $\nu = \Delta$ , so the corresponding shift is  $\delta\nu_{ac} \sim \gamma^2 / (4\Delta)$ . Hence for  $\gamma = 20$  kHz and transition frequencies  $\sim 3 - 1000$  MHz, the shift varies from  $\sim 0.1 - 30$  Hz. For the 3.1 MHz-transition, for which the shift is largest, the requirement on the amplitude stability necessary to achieve a sensitivity of a few mHz must be better than  $10^{-4}$ . However, this requirement becomes much less stringent at a for higher frequency transitions. For  $\nu \sim 1$  GHz, only a modest control at a level of a few percent is required.

We now consider frequency shifts due to all other levels on the transition frequency between levels  $m$  and  $n$ :

$$\delta\nu'_{ac} \approx \sum_{j \neq m} \frac{d_{mj}^2 E^2}{4(\Delta_{mj} - \nu)} - \sum_{k \neq n} \frac{d_{nk}^2 E^2}{4(\Delta_{nk} - \nu)}, \quad (6)$$

where  $d_{mj}$  is the dipole matrix element and  $\Delta_{mj} = E_m - E_j$  is the energy separation between levels  $m$  and  $j$ . We have ignored the Bloch-Siegert terms by assuming that  $\nu \approx \Delta_{mn}$ . For even isotopes, this shift is  $\sim 0.1$  Hz and is mostly determined by levels which are  $> 2000$   $\text{cm}^{-1}$  away with dipole matrix elements  $\sim 1$  ea<sub>0</sub>. A comparable shift occurs for odd isotopes, assuming a particular choice of hyperfine transitions for which  $\Delta_{mj} - \nu \sim 1$  GHz and  $d_{mj} \sim 4$  kHz/(V/cm). Thus, taking into account the shifts due to other levels does not lead to more stringent requirements on the amplitude stability of the rf electric field.

## C. Stray magnetic fields

The residual magnetic field ( $B$ ) can be controlled to  $\sim 1$   $\mu\text{G}$  in the magnetically shielded interaction region. This corresponds to Zeeman shifts  $g_F \mu_0 B \sim 1$  Hz, where  $\mu_0$  is the Bohr magneton and  $g_F$  is the Landé g-factor (Table II). If the Zeeman sublevels are equally populated but still unresolved, then this field does not shift the central frequency of a resonance lineshape but rather only broadens the lineshape with a corresponding width of  $\sim F(g_{FB} - g_{FA})\mu_0 B \approx 1$  Hz. However, an imbalance of sublevel populations can lead to asymmetric broadening of the resonance lineshape, causing an apparent shift in the central frequency. In the experimental geometry

TABLE II: g-values for the hyperfine levels of states A & B ( $g_{JA} = 1.21$  and  $g_{JB} = 1.367$ ).

F	$g_{FA}$	$g_{FB}$
7.5	1.57	1.77
8.5	1.36	1.54
9.5	1.22	1.38
10.5	1.11	1.26
11.5	1.03	1.16
12.5	0.968	1.09

(Fig. 3) discussed, such an imbalance may be caused by residual circular polarization coupled with misalignments of the propagation direction of the linearly polarized light beams used in the first and second step of the population. Because residual circular polarization can be controlled to the level of  $\sim 10^{-5}$  using standard polarimetric techniques, the shift of the resonance frequency can be made  $\ll 10^{-5}$  Hz.

## D. Millman effect in electric resonance

Misalignments of the atomic beam and the geometry of the electrodes can cause the direction of the rf E-field to rotate, as seen by a moving atom. This may lead to frequency shifts [21] analogous to the Millman effect encountered in magnetic resonance [22]. Let  $\Omega$  be the frequency of this apparent E-field rotation. Because an oscillating field can be decomposed into two counter-rotating components: one component is shifted by  $+\Omega$  and the other by  $-\Omega$ .

Using the measured homogeneity of our electric field, we estimate  $\Omega \lesssim 50$  Hz. However, for a resonance lineshape with unresolved sublevels, the central frequency remains largely unaffected. This is not true in the case of magnetic resonance (where transitions occur between magnetically split sublevels of the same level) and can be explained as follows: In the basis in which the quantization axis is perpendicular to the electric field, there are only  $\sigma_+$  and  $\sigma_-$  transitions. The Millman effect causes shifts in the frequencies of these transitions as illustrated in Fig. 5 for a  $\Delta J = 0$  transition on resonance (where we have assumed that the apparent electric field rotation is in the same sense as the  $\sigma_+$  component). If the sublevels of the initial state are equally populated and  $\Omega \ll \gamma$ , then these shifts only lead to a broadening of the lineshape. However, if there is an imbalance of sublevel populations the broadening is asymmetric, which can cause an apparent shift in the central frequency by an amount  $\sim \xi\Omega$ , where  $\xi$  is the degree of atomic orientation. As mentioned earlier, residual circular polarization in the linearly polarized light, used in the first and second step of

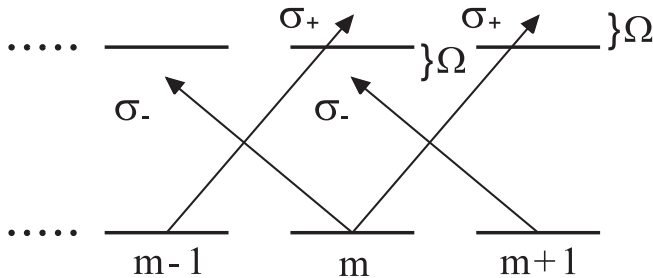


FIG. 5: Electric field frequency shifts due to the Millman effect.

the population, may induce atomic orientation, but can be controlled to the level of  $\sim 10^{-5}$ , which is sufficient for the desired sensitivity to  $\alpha$ . Furthermore, it should be noted that it is not the amplitude of the frequency shift but rather the stability that is important.

### E. Black-body radiation

Black-body radiation (BBR) can cause ac Stark shifts [23]. The rms value of the black-body radiation electric field is

$$\langle E^2 \rangle = (8.319 \text{ V/cm})^2 [T(\text{K})/300 \text{ K}]^4. \quad (7)$$

A shift in the transition frequency arises from the difference in the ac Stark shifts experienced by levels  $A$  and  $B$ . We can give a rough estimate of this Stark shift ( $\delta\nu_{BB}$ ) for one of these levels using Eq. (6):

$$\delta\nu_{BB} \sim \frac{d^2 \langle E^2 \rangle}{4(\Delta - \nu_{BB})}, \quad (8)$$

where  $\Delta$  is a characteristic atomic energy scale,  $\nu_{BB}$  is a characteristic frequency of room-temperature BBR, and  $d = 1 \text{ ea}_0$  is a typical optical transition dipole moment. Due to cancellations of contributions from nearby energy levels above and below the  $A$  and  $B$  levels, we assume that the net shift comes mainly from levels with large energy separations:  $\nu_{BB} \ll \Delta \sim 10^{14} \text{ Hz}$ , gives an estimate of  $\delta\nu_{BB} \lesssim 0.1 \text{ Hz}$ .

The interaction region is illuminated by much hotter BBR from the atomic oven ( $T \sim 1500 \text{ K}$ ) which is  $\sim 15 \text{ cm}$  away. However, the effect is smaller due to the decreased solid angle:

$$\begin{aligned} \delta\nu_{oven} &\sim \delta\nu_{BB} [T(\text{K})/300 \text{ K}]^4 \left( \frac{\Delta\Omega}{4\pi} \right), \\ &= 0.1 \text{ Hz} \left( \frac{1500 \text{ K}}{300 \text{ K}} \right)^4 \left( \frac{1 \text{ cm}^2}{4\pi \cdot 15^2 \text{ cm}^2} \right), \\ &= 0.02 \text{ Hz}, \end{aligned} \quad (9)$$

where we have assumed that an atom in the interaction region sees  $1 \text{ cm}^2$  of hot surface.

The BBR shifts are large compared to the desired level of sensitivity and are difficult to eliminate. However, these shifts can be kept constant to the desired level by stabilizing the temperature of the interaction region (to  $\sim 2 \text{ }^\circ\text{C}$ ) and the oven (to  $\sim 30 \text{ }^\circ\text{C}$ ). For the oven, possible changes in surface emissivity will be a concern and requires further investigation.

### F. Collisional shifts

Collisional shifts are typically  $\sim 1 - 10 \text{ MHz/Torr}$  for atomic E1 transitions. In the worst case scenario, to keep shifts below a few mHz, the residual gas pressure must be stable at a level  $\sim 10^{-10} \text{ Torr}$ . This can be achieved with standard UHV equipment. The pressure stability and composition of the residual gas will be monitored with a residual gas analyzer. However, we may find that collisional shifts are much smaller because the A-B transition is nominally between f and d inner-shell electrons [24]. In addition, quenching cross-sections, which effectively remove atoms from the beam, are expected to be large and so will reduce the effect of collisional shifts.

Another concern is collisional shifts due to Dy atoms themselves. In the absence of collisional quenching, the worst-case estimate is that the present Dy density ( $\sim 10^{10} \text{ atoms/cm}^3$ ) gives a shift of  $\sim 2 \text{ Hz}$ . This effect will be investigated and, if needed, the Dy beam intensity can be monitored and stabilized.

### G. Doppler Shift

The effect of the first-order Doppler shift is estimated to be small. To see this, we model the electric field (Fig. 3) as a standing wave constructed from two traveling waves propagating along the direction of the atomic beam. Due to ohmic losses within each electric-field plate, the amplitude of each wave gets attenuated. A difference in the power in these waves leads to asymmetric Doppler broadening of the lineshape, and thus an apparent shift. We estimate this difference by first considering the B-field induced by the time-varying E-field. This B-field persists inside the plates to within a skin-depth, inducing currents from which the power loss into the plates can be readily calculated [25]. We estimate the fractional power difference and, thus, the asymmetry to be  $\lesssim 10^{-4}$  for a transition frequency of  $1 \text{ GHz}$ . Since the Doppler width is  $\sim 2 \text{ kHz}$  at this frequency, the corresponding shift is  $\sim 0.2 \text{ Hz}$ . One can imagine a factor of  $\sim 10$  suppression if rf power is fed to the plates in a symmetric fashion. Thus, this shift is only required to be stable to  $\sim 10\%$  in order to achieve a sensitivity of a few mHz.

Likewise, depending upon the rf transition, the second order Doppler shift is  $\sim 10^{-3} - 10^{-6} \text{ Hz}$ , which is sufficiently small.

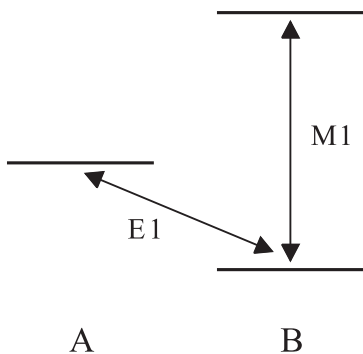


FIG. 6: Simultaneous measurement of an M1 transition frequency for a nonzero nuclear spin isotope facilitates the control of systematics.

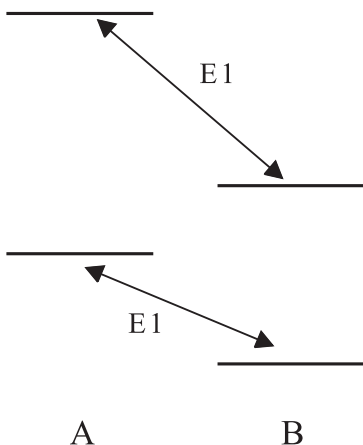


FIG. 7: Simultaneous measurement of two (or more) E1 transition frequencies to facilitate the control of systematics. This method works with the two zero-spin isotopes,  $^{162}\text{Dy}$  and  $^{164}\text{Dy}$ .

#### H. Techniques to control systematics

A powerful method to detect and eliminate possible sources of systematic shifts common to both levels is to

simultaneously measure the transition frequency between hyperfine levels of a given parity state. The reason is that, because the levels involved have the same relativistic corrections, this frequency is insensitive to variations of  $\alpha$ . One possible scheme is to excite an M1 transition, e. g., as shown in Fig. 6, whose frequency can be monitored by looking for disappearance in the fluorescence from level A for a fixed E1 transition frequency. Alternatively, we can utilize another E1 transition as shown in Fig. 7. In this scenario,  $\alpha$  variation is twice as large in the sum of the two frequencies, while the difference is insensitive to  $\alpha$  variations.

Furthermore, one can compare E1 transitions for the two abundant isotopes with zero nuclear spin ( $^{162}\text{Dy}$  and  $^{164}\text{Dy}$ ). The counting rate is significantly higher and the level structure is much simpler without hyperfine interactions.

## V. DISCUSSION

In summary, rf E1 transitions in Dy provide an attractive system in which to test the temporal variation of  $\alpha$ . The frequencies of these transitions can be directly counted. For a limit of  $\dot{\alpha}/\alpha < 10^{-15}/\text{yr}$ , the shift was calculated to be  $\approx 2 \text{ Hz/yr}$ . At present, a statistical sensitivity of 0.6 Hz in one second of integration time is achievable. Knowledge of systematic effects are critical to this experiment. Preliminary analysis shows that they can be controlled to a level corresponding to  $|\dot{\alpha}/\alpha| \sim 10^{-18}/\text{yr}$ , a level of sensitivity that would rival that of the most stringent observational limit set by the Oklo natural reactor.

#### Acknowledgments

We thank D. F. Kimball, M. G. Kozlov, J. E. Stalnaker, and V. V. Yashchuk for valuable discussions. This work was supported in part by the UC Berkeley-LANL CLE program. D. B. also acknowledges the support of the Miller Institute for Basic Research in Science.

- 
- [1] J. Uzan, *Rev. Mod. Phys.* **75**, 403 (2003).
  - [2] W. Marciano, *Phys. Rev. Lett.* **52**, 489 (1984).
  - [3] J.D. Barrow, *Phys. Rev. D* **35**, 1805 (1987).
  - [4] T. Damour and A.M. Polyakov, *Nucl. Phys.* **B423**, 532 (1994).
  - [5] T. Damour, F. Piazza, and G. Veneziano, *Phys. Rev. Lett.* **89**, 081601 (2002).
  - [6] J. K. Webb, *et al.*, *Phys. Rev. Lett.* **87**, 091301 (2001).
  - [7] A.I. Shlyakhter, *Nature* **264**, 340 (1976).
  - [8] T. Damour and F. Dyson, *Nucl. Phys.* **B480**, 37 (1996).
  - [9] Y. Fujii, *et al.*, *Nucl. Phys.* **B573**, 377 (2000).
  - [10] C. Salomon, *et al.*, *AIP Conf. Proc.* **551**, 23 (2001).
  - [11] J. D. Prestage, R. L. Tjoelker, and L. Maleki, *Phys. Rev. Lett.* **74**, 3511 (1995).
  - [12] S. Bize, *et al.*, *Phys. Rev. Lett.* **90**, 150802 (2003).
  - [13] V. A. Dzuba, V. V. Flambaum, and J. K. Webb, *Phys. Rev. Lett.* **82**, 888 (1999).
  - [14] V. A. Dzuba, V. V. Flambaum, and J. K. Webb, *Phys. Rev. A* **59**, 230 (1999).
  - [15] V. A. Dzuba, V. V. Flambaum, and M. V. Marchenko, (2003) e-print physics/0305066 at <http://arxiv.org/>.
  - [16] D. Budker, D. DeMille, E. D. Commins, and M. S. Zolotarev, *Phys. Rev. A* **50**, 132 (1994).
  - [17] A. T. Nguyen, G. D. Chern, D. Budker, and M. Zolo-

- torev, Phys. Rev. A **63**, 013406 (2000).
- [18] A. T. Nguyen, D. Budker, D. DeMille, and M. Zolotarev, Phys. Rev. A **56**, 3453 (1997).
- [19] V. A. Dzuba (private communication).
- [20] W. Itano, J. Res. Natl. Inst. Stand. Technol., **105**, 829 (2000).
- [21] L. Grabner and V. Hughes, Phys. Rev. **70** 819 (1950).
- [22] S. Millman, Phys. Rev. **55**, 628 (1939).
- [23] V. G. Pal'chikov, Y. S. Domnin, and A. V. Novoselov, J. Opt. B **5**, S131 (2003).
- [24] V. D. Vedenin and V. N. Kulyasov, Opt. Spectroc. (USSR) **59**, 603 (1985).
- [25] J. D. Jackson. *Classical Electrodynamics, 2nd. ed.* (John Wiley & Sons, New York, 1975).